A spatiotemporal adaptive local search method for tracking congestion propagation in dynamic networks

Abstract

The cascading effect of traffic congestion propagation can cause large-scale disruptions to networks. Existing studies have laid a solid foundation for characterizing traffic congestion propagation. However, they are either based upon certain traffic flow theory assumptions or rely on predefined graph structures, resulting in distortion problems or downgraded accuracy in practice. To address these limitations, we propose a spatiotemporal adaptive local search (STALS) method, which feeds the dynamically updated adjacency matrices into local search algorithm, instead of predefining them. Specifically, the STALS is composed of two data-driven modules. Dynamic adjacency matric learning module learns the spatiotemporal relationship from varying congestion graphs by fusing node curvature, node degree, spatial proximity, and semantic information. Local search module introduces local dominance to track the propagation of traffic congestion by identifying multi-scale communities. We test our proposed method on the four benchmark networks with an average of 15,000 nodes at five snapshots. The STALS remains an NMI score level at approximately 0.97 and an average execution time of 27.66s, while the six competing state-of-the-art methods exhibit sensitivity to robustness or inferior efficiency. We also apply the STALS to two large-scale traffic networks in New York City, the United States, and Shanghai, China. An ablation study reveals that the combination of four features achieves the highest modularity of 0.85. A comparative analysis on the two datasets validates the efficacy of the STALS in revealing the distinctive traffic congestion propagation mechanisms in both metropolitan areas.

Keywords: Traffic congestion, Adjacency matrix, Local dominance, community detection, Congestion propagation

1. Introduction

Traffic congestion is a byproduct and inevitable result of increasing urbanization. The cascading effect

(Basak et al., 2019) of traffic congestion propagation can trigger secondary and tertiary congestion, because it propagates in dynamic traffic networks from the congestion source regardless of recurrent and non-recurrent congestion (Anbaroglu et al., 2014). This can cause severe operational issues including prolonged traffic delays, increase urban pollution, and heightened energy consumption, thus imposing challenges on traffic management (Lu et al., 2021; Wang et al., 2021). From this perspective, exploring the root causes and unraveling the propagation laws of traffic congestion show practical significance.

To achieve this goal, great efforts have been made in primary two aspects. The first one focuses on traffic congestion source identification. Wright and Roberg (1998) attributed congestion source to bottlenecks and categorized traffic bottleneck into three types, which are caused by random incidents, network capacity, and surging travel demand in specific areas. Based on this concept, previous studies put significance into the formation and detection methods of highway bottlenecks, which can be traced back to the continuum model (i.e., LWR proposed by Lighthill and Whitham (1955) and Richards (1956)) of traffic flow. The main idea is to use the quantified traffic states and estimated congestion indices as the decision-making basis to determine the bottleneck. Compared with highway, the complex properties (e.g., traffic control, road structure constraints) of urban roadways added challenges to its congestion bottleneck identification. Overall, existing studies mainly yield three key research findings: (i) comprehensive summary of the causes for congestion bottlenecks, including certainty and uncertainty factors; (ii) the impacts of congestion bottlenecks and their relationship with road network accessibility; (iii) some bottleneck identification methods for small-scale networks.

The second one attaches importance to traffic congestion propagation modeling, primary including two branches: simulation-driven and measured data-driven methods. Microscopic simulation takes vehicles as research object and transforms the propagation process as a queuing problem. Representative mathematical models include car-following (Gipps, 1981) and lane-changing (Laval and Daganzo, 2006). However, the microscopic approach may suffer from distortion problem and is difficult to apply to large-scale networks. On the contrary, macroscopic simulation directly utilizes the traffic flow parameters to characterize its propagation process. Especially, cell transmission model (CTM) (Daganzo, 1994 and 1995)

and its variants have received attention in recent years (Levin and Boyles, 2016; Long et al., 2011). Considering the similarity between congestion diffusion and disease spreading, some scholars also introduced the susceptible-infectious-recovered (SIR) model into this process (Wu et al., 2004; Saberi et al., 2020). However, the macroscopic approach relies on underlying models and oversimplifies the traffic network. To reply this, measured data-driven method utilizes real traffic data to infer congestion propagation. Especially since the 21st century, the explosive growth of multi-source, real-time geographic data with temporal and spatial information has powered the application of machine learning in this field. This method can be divided into two categories: dynamic Bayesian network (DBN) (Sun et al., 2015) and deep learning models (Ang et al., 2022). Most DBN-based approaches discretize continuous historical data into several traffic states and then calculate the state transition probability between two adjacent road segments, thus inferring congestion propagation patterns (Chen et al., 2018; Fan et al., 2019; Nguyen et al., 2016). However, data discretization and prior knowledge affect the inference effectiveness. Different from these works, deep learning models construct feature matrices based on road network topology, including graph neural network (GNN) (Wu et al., 2020), graph convolutional network (GCN) (Kipf and Welling, 2016), and their variants (Zheng et al., 2022).

Despite the fruitful results, critical challenges still remain: (i) GNNs and GCNs usually rely on a predefined road network adjacency matrix, which is calculated based on node connectivity or spatial proximity. However, Jiang and Luo (2022) highlighted the superiority of dynamic matrix over the pre-defined matrix, which offers more flexibility and adaptability in capturing spatiotemporal dependency. (ii) The effectiveness of measured data-driven method highly relies on the spatiotemporal resolution of collected data, as it seeks to reveal large-scale traffic dynamics by obscuring small-scale spatiotemporal interactions (Xiong et al., 2023).

The above challenges prompt the proposal of a spatiotemporal adaptive local search (STALS) method, which dynamically updates adjacency matrices from continuously evolving traffic data. This inspiration is motivated by Saberi et al. (2020) - traffic systems exhibit underlying spreading dynamics similar to those observed in other complex systems, e.g., social networks, population contact networks, or technological

networks. And Shi et al. (2024) declared that communities or clusters can provide a coarse-grained description of complex systems at multiple scales. In this light, the proposed method tracked traffic congestion propagation at the level of community structure, consisting of two data-driven modules - dynamic adjacency matrix learning module for multi-feature fusion and local search module for community detection. Experiments on four benchmark datasets demonstrate that the STALS outperforms the six competing state-of-the-art models. The contribution lies in three folds:

- A dynamic adjacency matrix is designed which is adaptive to data at different time granularities and could automatically capture the multiple features (i.e., node curvature, node degree, spatial proximity, and semantic information) varying over the spatiotemporal congestion graphs.
- The proposed method is the first to extend community detection to traffic congestion propagation modelling by introducing the concept of local dominance, which offers a new perspective for understanding the complex propagation dynamics.
- A comparative analysis on the two real-world traffic congestion sceneries in large-scale networks validates the successful application of our proposed method for revealing the distinctive traffic congestion propagation mechanisms in both metropolitan areas.

2. Related works

Unraveling the evolution mechnisms of congestion in the road network is key to traffic congestion propagation analysis. Existing studies have made great efforts for this purpose, primarily including two categories (**Fig. 1**): simulation-driven and measured data-driven methods.

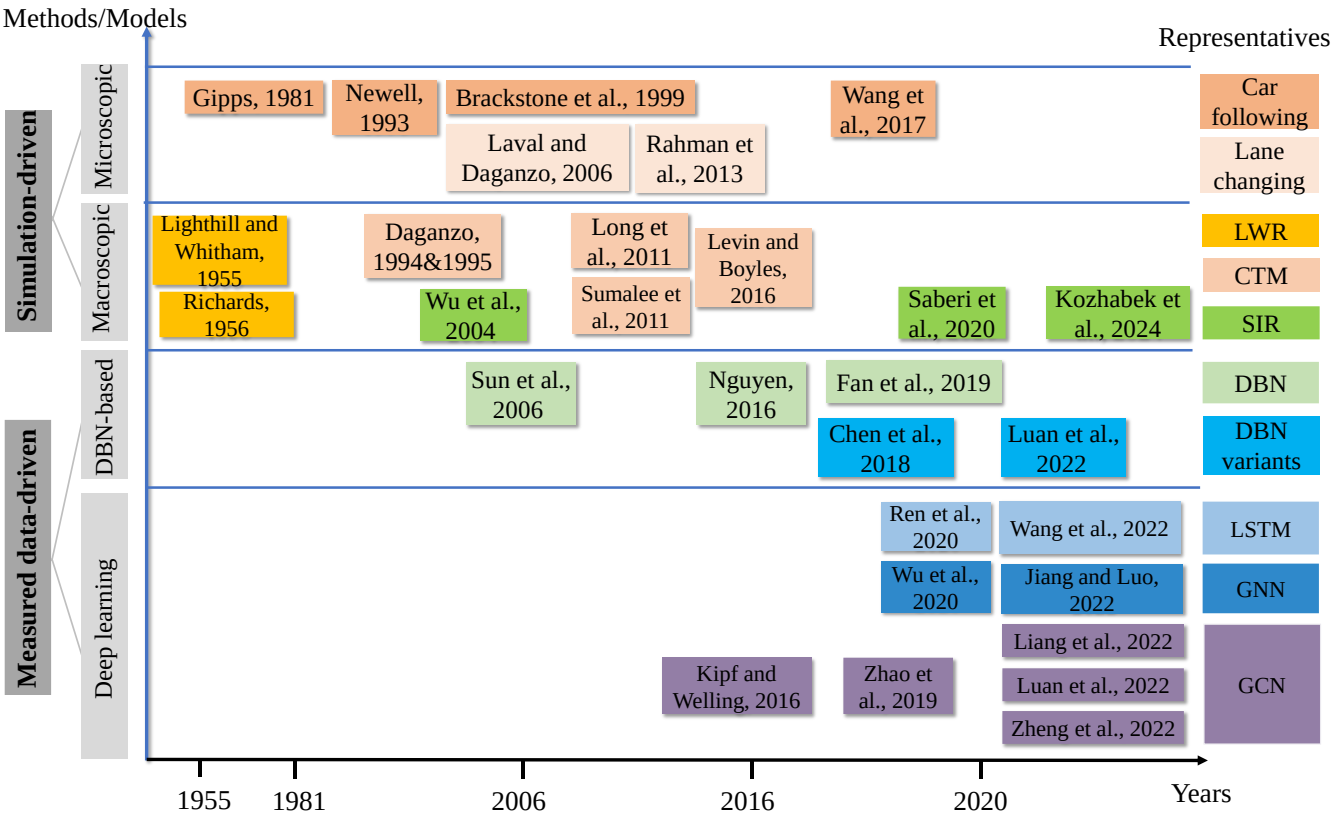

Fig.1. Literature review of traffic congestion propagation analysis methods, models, and representatives.

2.1. Simulation-driven method

Simulation is a mainstream means to study the characteristics of traffic congestion. By constructing platforms and simulating dynamic traffic flow in road networks, it has been earlier applied to describe congestion propagation process. According to different research objects, this method can be divided at microscopic and macroscopic scales.

Microscopic models take each vehicle as the basic research unit and regard traffic flow as a system composed of self-driven particles. They are mainly dominated by car-following and lane-changing theories. Car-following theory transforms traffic congestion propagation process into queuing problem (Newell, 1993), which focuses on the distance to the front vehicle and has spawned several variations (Brackstone al., 1999; Wang et al., 2017). However, it cannot take into account the individual differences in vehicles, such as vehicle types, driver behavior, and others. Lane-changing theory is more suitable for describing complex traffic scenarios than car-following, as it considers driver distraction, environmental and geometric

factors (Rahman et al. 2013). Despite this, both car-following and lane-changing modelling oversimplify traffic network, resulting that they cannot be applied to large-scale networks.

Macroscopic models focus on the overall characteristics of traffic flow. Representative models include the LWR, CTM, and SIR. The LWR model (Lighthill and Whitham, 1955; Richards, 1956) utilizes partial differential equations to analyze the relationship among three traffic parameters (volume, density, and speed), laying a foundation for many other macroscopic models. Daganzo (1994) first established the CTM by discretizing and finite-differentiation the LWR model, which divides road network into discrete and finite cells evolving with certain rules. Subsequently, many CTM variants of have emerged for specific purposes. For example, Long et al. (2011) improved the CTM to explore the impacts of multiple factors on traffic congestion propagation and dissipation under emergencies. Sumalee et al. (2011) further developed a stochastic CTM (SCTM) to describe the macroscopic dynamics of the traffic flow under demand and supply uncertainties. Despite this, CTM-based models require a fixed cell length, which makes it difficult to adapt to urban road systems with highly irregular geometric conditions. Different from these works, Wu et al. (2004) conjectured that traffic congestion propagation can be described with a SIR model, but did not provide empirical validation. Based upon this, Saberi et al. (2020) and Kozhabek et al. (2024) validated the dynamics of congestion propagation and dissipation through multi-city analysis by using the proposed SIR-based framework.

Although the simulation-driven method can vividly describe the dynamic characteristics of traffic flow, it has several drawbacks: (i) both microscopic and macroscopic methods require certain traffic flow theory assumptions and rely on underlying models; (ii) Excessive model parameter calibration may cause "distortion" problems; (iii) It may be difficult to extend to large-scale networks or complex traffic sceneries, limiting its application scope.

2.2. Measured data-driven method

In view of the limitations of simulation-driven method, measured data-driven method aided by the location-acquisition technologies has gradually received more attention. This method prioritizes the inference or prediction of traffic propagation patterns by analyzing the spatiotemporal dependency or

heterogeneity. One important branch is DBN, which regards congestion propagation between two adjacent road segments as the state transition of two nodes in a probabilistic graph (Sun et al., 2006). Nguyen et al. (2016) built causal congestion trees in the DBN based on taxi trajectory data to estimate causality probability and reveal the causal interactions of traffic streams. Based upon this, Chen et al. (2018) proposed the space-temporal congestion subgraph (STCS) based on travel time data to describe congestion propagation and reveal the recurring congestion propagation patterns. Fan et al. (2019) established a DBN prediction model to predict the congestion diffusion states based on floating car data by discretizing traffic speed. However, the effectiveness of DBN-based approaches relies on prior knowledge.

The other branch is deep learning, which regards congestion propagation attributes as multi-dimensional features, thus constructing matrices for predictive purpose. Representative traditional models include such as LSTM (Ren et al., 2020), bidirectional LSTM (Wang et al., 2022), and generative adversarial networks (Zhang et al., 2019). Despite great advantages, they fail to consider the road network topology and may result in unsatisfactory performance. The proposal of GCN addresses this defect, which directly regards traffic network as a graph and road segments as nodes in the graph (Kipf and Welling, 2016). Since then, GCN and GCN variants have been widely used for traffic congestion propagation prediction in large-scale networks. For example, temporal GCN (T-GCN) was proposed by Zhao et al. (2019) to capture both spatial and temporal dependences. Spatio-temporal GCN (ST-GCN) simultaneously captures spatiotemporal dependences and heterogeneity (Liang et al., 2022). Dynamic STGCN (DST-GCN) constructed the spatial-temporal graph across time slices by connecting the latest time slice with each past time slice (Zheng et al., 2022). Interestingly, Luan et al. (2022) proposed a dynamic Bayesian graph convolutional network (DBGCN) by integrating Bayesian inference into deep learning.

Despite the great efforts, critical challenges still exist in congestion propagation analysis based on measured-driven method: (i) Both DBN-based and GNN-based approaches require predefined knowledge (e.g., a predefined road network adjacency matrix). However, the propagation mechanism of traffic congestion is far more complicated than road network topology. (ii) Temporal resolution (e.g., 5min, 30min, 1h) and spatial resolution (e.g., grid-based, road-based, zip-code-based partitions) of the data affect model

effectiveness.

3. Methodology

3.1. Preliminary definitions

3.1.1. Spatiotemporal congestion instance

Traffic State Index (TSI) (Chen et al., 2018) is adopted to measure the traffic state in this study. Given a road segment f_i at the timestamp t_j, the TSI is calculated by the relative deviation rate of actual speed to the free-flow speed:

$$TSI_{f_i,t_j} = \frac{v_{f_i} - \bar{v}_{f_i,t_j}}{v_{f_i}}, \quad (1)$$

where v_{f_i} represents the free-flow speed or road segment f_i, $\bar{v}_{f_i,t_j}$ is the actual average speed at timestamp t_j. The range of TSI_{f_i,t_j} is [0,1], and the threshold is 0.7 (Chen et al., 2018). Therefore, the road segment f_i at the timestamp t_j is defined as a spatiotemporal congestion instance if its TSI_{f_i,t_j} is no less than 0.7.

3.1.2. Spatiotemporal congestion subgraph

A spatiotemporal congestion subgraph $G_{t_j}(V_{t_j}, E_{t_j}, W_{t_j})$ is defined as the set of all spatiotemporal congestion instances at the timestamp t_j, where $V_{t_j}, E_{t_j}, W_{t_j}$ represent nodes, edges, and weights, respectively. The nodes in the subgraph represent congested road segments, and the weights of edges are determined by the spatiotemporal relationship between adjacency nodes. A set of spatiotemporal congestion subgraphs for sequential time periods is termed as a spatiotemporal congestion graph:

$$G = \bigcup_{j=1}^{J} G_{t_j}(V_{t_j}, E_{t_j}, W_{t_j}), \quad (2)$$

where J is the total number of timestamps.

3.1.3. Spatiotemporal adjacency relationship

The edge values of $G_{t_j}(V_{t_j}, E_{t_j}, W_{t_j})$ are measured by the spatiotemporal relationship between two adjacency nodes. Although nodes are fixed by certain physical constraints, their relationship changes dynamically over time and evolving spatiotemporal congestion subgraphs. In this study, we capture this relationship for each spatiotemporal congestion subgraph from four aspects: node geometry, node topology,

spatial proximity, and semantic information.

- Node geometry. Existing studies have shown curvature is a key structural property for characterizing large-scale networks and has a major impact on core congestion (Narayan and Aaniee, 2011). Inspired by this, we calculated the curvature of each road segment as node geometry.
- Node topology. The degree of a node is an important concept that affects information diffusion and the stability of graph structure. It refers to the number of edges directly connected to the node. Notably, nodes with higher degrees are considered with higher centrality in the network.
- Spatial proximity. Spatial proximity is a significant indicator for measuring the spatiotemporal dependency in a graph, which can effectively reflect the interaction between nodes. According to Jiang and Luo (2022), spatial proximity mainly contains two sub-types, namely neighbor closeness and distance closeness. In this study, we choose distance closeness (i.e., Euclidean distance), since node degree has already captured neighbor proximity to some extent.
- Semantic information. Semantic information offers additional dynamic knowledge beyond graph structure, e.g., spatiotemporal dependency learned from the TSI time series. According to Alam et al. (2014), fast Fourier transform can effectively extract the inherent nature of time series characteristics and eliminate the effects of temporal resolution. Inspired this, fast Fourier transform of the TSI matrix is adopted to capture dynamic traffic state information in this study.

3.2. Framework of STALS

We propose a new data-driven method, namely STALS, for tracking congestion propagation in dynamic networks at the level of community structure. The STALS calculated dynamic adjacency matrices instead of predefined ones by fusing four features (i.e., node curvature, node degree, spatial proximity, and TSI semantics). The framework of the proposed method contains two-driven modules (**Fig. 2**): dynamic adjacency matrix learning module, and local search module for community detection. More specifically, the adaptive adjacency matrices designed from traffic spatiotemporal congestion graphs (Section 3.2.1) are fed into the local search algorithm (Section 3.2.2), where the multi-scale communities can be detected.

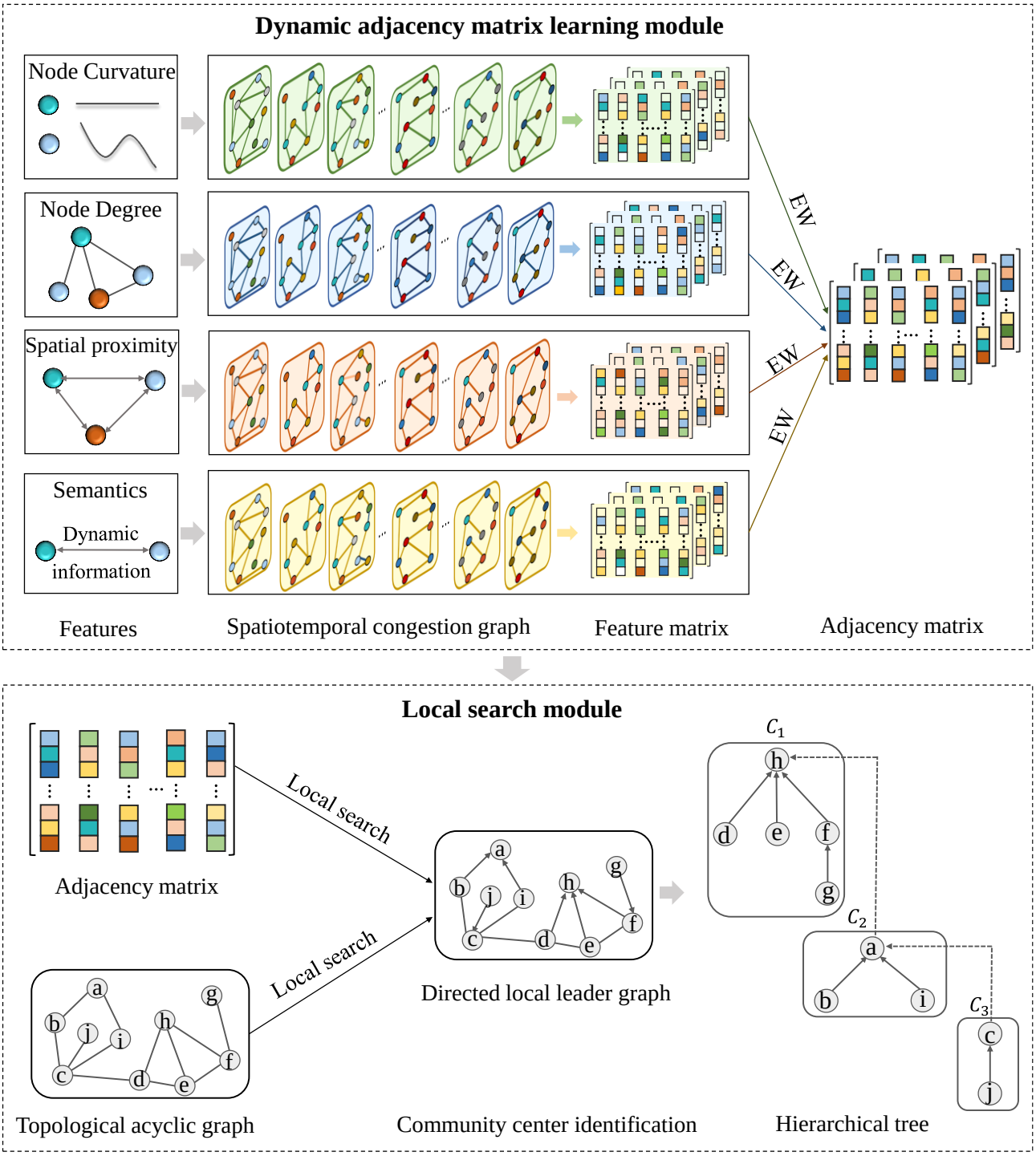

Fig. 2. Framework of the proposed method.

3.2.1. Dynamic adjacency matrix learning

Entropy weight (EW) is conducive to increasing the dipartite degree of the relative closeness in multi-attribute decision-making (Chen 2021). Considering this merit, the EW approach is adopted to calculate adaptive adjacency matrices in this study. Given a spatiotemporal congestion subgraph G_{t_j} at timestamp t_j, its adaptive adjacency matrix M_{t_j} is calculated as the weighted fusion of its curvature similarity K_{t_j}, degree

similarity D_{t_j}, Spatial proximity similarity S_{t_j}, and Fourier transform of traffic state similarity F_{t_j}:

$$M_{t_j} = w_{t_j,1}K_{t_j} + w_{t_j,2}D_{t_j} + w_{t_j,3}S_{t_j} + w_{t_j,4}F_{t_j} \tag{3}$$

where $w_{t_j,1}$, $w_{t_j,2}$, $w_{t_j,3}$, and $w_{t_j,4}$ represent the EWs calculated by the information entropy of each similarity matrix. Given a spatiotemporal congestion graph G, its adjacency matrices at J timestamps can be automatically updated as $M = [M_{t_1}, M_{t_2}, \dots, M_{t_J}]$.

3.2.2. Local search algorithm

Based upon the adaptive adjacency matrices, a local search algorithm is employed to detect multi-scale communities in dynamic networks. The process of local search in this study is shown as the local search module in **Fig. 2**, which can be broken into the following four stages.

The first step involves attributing a value x_u to each node u in the network. This is achieved by combining the adjacency matrix from the dynamic adjacency matrix learning module with the topological graph obtained from the spatiotemporal congestion graph. Specifically, x_u is calculated by summing the values of all the edges that are directly adjacent to the node. This process enables the construction of a directed acyclic graph, where each node u points to its largest-value-neighbor v if the following conditions are met: (i) The node has a higher value than its neighbor, i.e., $x_u \leq x_v$, and (ii) each node u pointing to its largest-value-neighbor, i.e., $x_v = max\{x_i | i \in V(u)\}$, where $V(u)$ represents the set of all neighbors of u. The second stage involves identifying local leaders (Blondel et al., 2008a) for each graph based on the concept of local dominance. Local dominance refers to a leader-follower relationship in community structures, where nodes with incoming edge(s) but no outgoing edges are considered local leaders that dominates their surrounding area (see nodes a, c, and h in the module). These local leaders are crucial in understanding the network's hierarchical structure. Thirdly, for each local leader u, a local breath-first searching (LBFS) (Shi et al., 2024) algorithm is employed to find its nearest local leader v with $x_u \leq x_v$. The advantage of the LBFS lies in its high efficiency, as it can terminate its search once a nearest local leader is identified, without traversing the entire network. And it can also enable the determination of the shortest path length between local leaders, providing valuable insights into the network's connectivity.

Finally, multi-scale communities denoted as the symbol C-*i* in the following text can be identified, with *i* symbolizing different levels and scales of communities.

4. Experiments

4.1. Datasets

4.1. Benchmark networks

To evaluate the performance of the STALS, four artificially generated networks derived from the benchmark datasets (i.e., Birthdeath, Expandcontract, Hide, and Mergesplit) are employed in this study. These synthetic networks were created by extending the static Lancichinetti-Fortunato Radicchi (LFR) benchmark (Lancichinetti and Fortunato, 2009) at five snapshots, allowing for the simulation of various community evolution patterns over time. For each snapshot, the true labels of communities are available. The four synthetic networks share common properties: an average node degree of 20, a maximum node degree of 40, and a community overlap parameter of 0.2. Additionally, at each time step, 20% of the nodes switch their community affiliations, reflecting the dynamic nature of community membership in real-world networks. These synthetic networks were specifically designed to capture all possible community evolution scenarios.

4.2. Real-world networks

To learn the traffic congestion propagation mechanisms, two real-word traffic networks from New York City (NYC), the United States, and Shanghai, China are adopted:

- NYC floating car data was downloaded from Uber Movement, covering a time period from December 1, 2018 to December 31, 2018. The time interval is 1 hour. Each record contains recording time, road segment ID, and average speed. The free-flow speed is also acquired from the Uber Movement. According to the data description of Uber Movement, the free-flow speed of a road segment equals to the 15th percentile value of the actual speeds of all floating vehicles, with speeds sorted in descending order. Therefore, a 24-dimensional time series feature over one day can be obtained.

- Shanghai taxi trajectory data was automatically collected by sensors, covering a time period from April 1, 2016 to April 30, 2016. The data collection interval is 5 seconds. Each record contains recording time, road segment ID, and actual speed. To compare with the NYC floating car data at different temporal resolutions, we aggregate the Shanghai taxi trajectory data into 5-minute intervals. And the calculation method of free-flow speed keeps consistent with that of Uber Movement. In this way, a 288-dimensional time series feature over one day can be obtained.

4.2. Experiments on the benchmark datasets

4.2.1. State-of-the-art methods

Most existing studies first detect static communities at each timestamp, and then adopted different similarity metrics to measure the relationship between two communities from different timestamps. In this study, six state-of-the-art approaches with different similarity measurements are set as the baselines compared with the STALS. To ensure the fairness, Louvain algorithm (Blondel et al., 2008b) are applied to detect static communities for each method.

- Heuristic threshold-based method (Green et al., 2010) first detected static communities at each timestamp, and then the detected communities were matched with each dynamic network's front community. The matching process was performed by calculating the Jaccard coefficient (Jaccard, 1912):

$$sim\left(C_{t_i}, C_{t_j}\right) = \frac{|C_{t_i} \cap C_{t_j}|}{|C_{t_i} \cup C_{t_j}|}, \tag{4}$$

where C_{t_i} and C_{t_j} represent two detected communities at timestamp t_i and t_j, respectively. The symbol | | represents the member numbers. C_{t_i} and C_{t_j} are considered as a matched community if $sim(C_{t_i}, C_{t_j})$ is larger than a threshold k. Experiments demonstrated that the optimal k was equal to 0.1.

- Text mining threshold-based method (Takaffoli et al., 2011) adopted a different similarity measurement to identify critical events in both consecutive and non-consecutive timestamps:

$$sim\left(C_{t_i}, C_{t_j}\right) = \begin{cases} \dfrac{|C_{t_i} \cap C_{t_j}|}{max\left(|C_{t_i}|, |C_{t_j}|\right)}, if \ \dfrac{|C_{t_i} \cap C_{t_j}|}{max\left(|C_{t_i}|, |C_{t_j}|\right)} \geq k \\ 0, \quad otherwise \end{cases} \tag{5}$$

Experiments illustrated that the optimal threshold k was equal to 0.3.

- Group evolution discovery (GED) (Brodka et al. 2013) introduced topological metric to optimize the defects of the former two methods that solely relied on similarity metric to track community evolution:

$$sim\left(C_{t_i}, C_{t_j}\right) = \frac{|C_{t_i} \cap C_{t_j}|}{|C_{t_i}|} \cdot \frac{\sum_{C \in \left(C_{t_i} \cap C_{t_j}\right)} NI_{C_{t_i}(f_i)}}{\sum_{C \in \left(C_{t_i}\right)} NI_{C_{t_i}(f_i)}}, \tag{6}$$

where $NI_{C_{t_i}(f_i)}$ represents the weight of node f_i within the community C_{t_i}, which can be measured in various centrality metrics, e.g., betweenness centrality, degree centrality. Experiments presented the optimal k was 0.1.

- Transition probability vector-based method (Tajeuna et al. 2015) utilized transition probability vectors to represent the degree of shared nodes between communities at different timestamps:

$$sim\left(C_{t_i}, C_{t_j}\right) = \begin{cases} \sum_{f_i}^{N_c} 2\dfrac{p_{C_{t_i},f_i} \cdot p_{C_{t_j},f_i}}{p_{C_{t_i},f_i} + p_{C_{t_j},f_i}}, & if \sum_{f_i}^{N_c} 2\dfrac{p_{C_{t_i},f_i} \cdot p_{C_{t_j},f_i}}{p_{C_{t_i},f_i} + p_{C_{t_j},f_i}} > k \\ 0, \quad otherwise \end{cases} \tag{7}$$

where N_c is the total number of communities in within the dynamic networks. $p_{C_{t_i},f_i}$ and $p_{C_{t_j},f_i}$ represent the components of the transition probability vectors $v_{C_{t_i}}$ and $v_{C_{t_j}}$. The threshold is automatically determined as the intersection point of two Gamma curves derived from similarity values between transition probability vectors.

- Identification of community evolution by mapping (ICEM) (Mohammadmosaferi et al., 2020) utilized a harsh-map to map the nodes in communities into a pair, which consists of a timestamp and a community index. Similarity of two communities was defined as:

$$sim\left(C_{t_i}, C_{t_j}\right) = \frac{|C_{t_i} \cap C_{t_j}|}{|C_{t_i}|}, \tag{8}$$

$$sim\left(C_{t_j}, C_{t_i}\right) = \frac{|C_{t_i} \cap C_{t_j}|}{|C_{t_j}|}, \tag{9}$$

where $t_i < t_j$. Communities C_{t_i} and C_{t_j} are considered partially similar if $sim(C_{t_i}, C_{t_j}) > k_1$ and $sim(C_{t_j}, C_{t_i}) > k_1$. And they are very similar if $sim(C_{t_i}, C_{t_j}) > k_2$. Experiments proved the optimal k_1 was 0.1 and the optimal k_2 was 0.5.

- Overlap coefficient-based method (Mazza et al., 2023) adopted an overlap coefficient to measure the similarity between communities:

$$sim\left(C_{t_i}, C_{t_j}\right) = \frac{|C_{t_i} \cap C_{t_j}|}{min\left(|C_{t_i}|, |C_{t_i}|\right)}, \tag{10}$$

4.2.2. Comparison results

Normalized mutual information (NMI) is employed to evaluate the detected communities with the ground-truth communities, which is defined as:

$$NMI\ (X,Y) = \frac{2 * I(X,Y)}{H(X) + H(Y)}, \tag{11}$$

where $H(X)$ and $H(Y)$ represent entropy of the detected communities and the ground-truth communities, respectively. $I(X,Y)$ represents mutual information of X and Y. The closer the NMI value is to 1, the more accurate community detection.

Fig. 3 compares the NMI of our proposed method with the six state-of-the-art methods on the four benchmark datasets. The exact NMI values are shown in **Appendix Tables 1-4**. The results show that our proposed method secures high NMI values for each dataset, although Greene and Mazza occasionally obtains slightly higher values (difference less than 0.05). More specifically, the STALS, Mazza, Greene, ICEM, and Tajeuna performs well on the former three datasets, while GED and Tajaffoli show relatively inferior effect. Notably, our proposed method remains an NMI score level above 0.97, and displays an upward trend with the snapshot growing. For the Mergesplit dataset, almost all methods exhibit their worst results and the NMI scores show a downward trend over snapshots. This can be attributed to the damage to the community structure cause by mergers and splits, making it more challenging to track multi-scale communities. Despite this, our method can still maintain an NMI score level over 0.95, demonstrating the robustness of the STALS. Overall, our proposed method demonstrates greater resilience in tracking communities as the network structure evolves, whereas some competing methods may exhibit growing

susceptibility to community matching inaccuracies over snapshots.

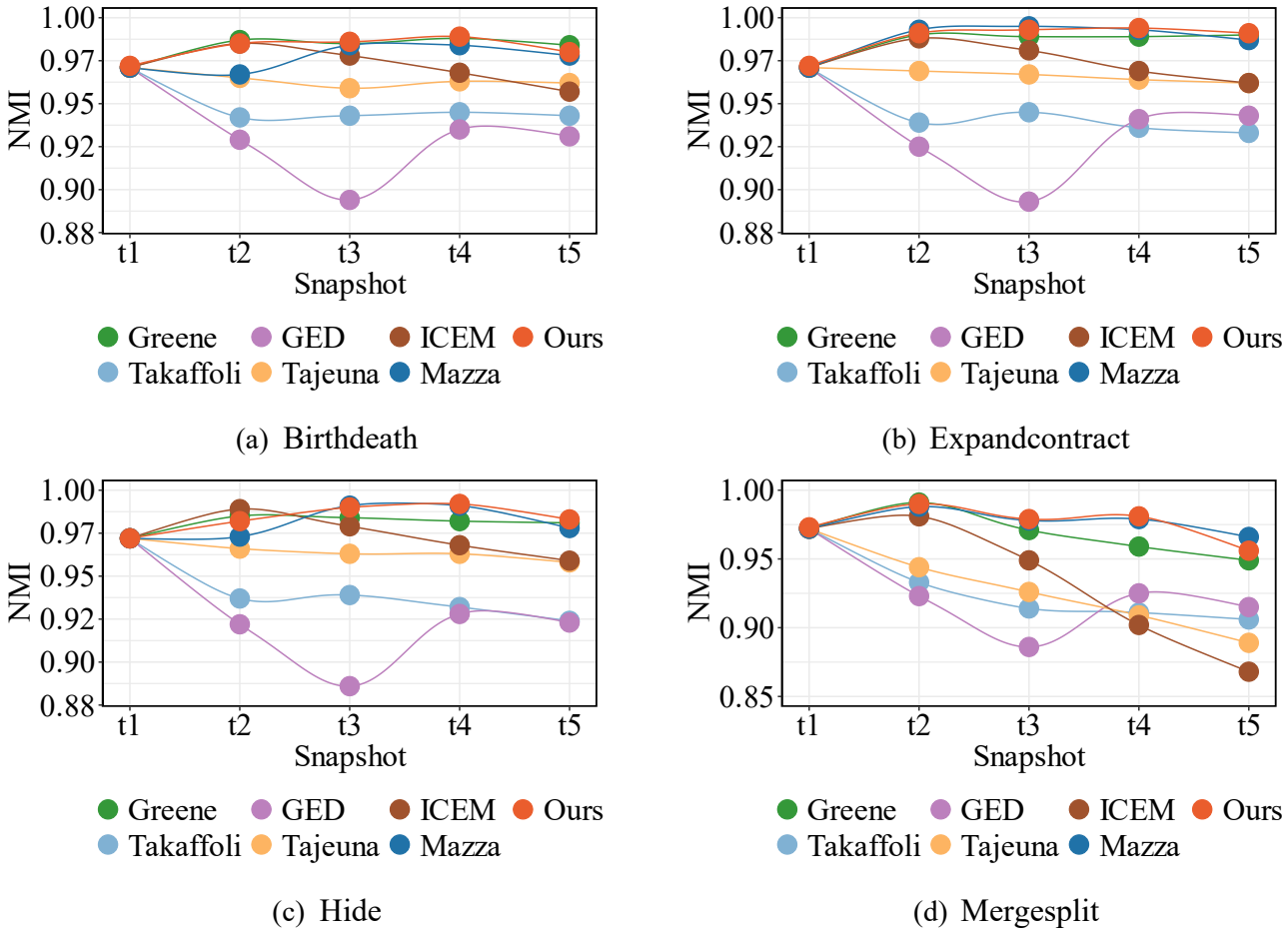

Fig. 3. NMI of the proposed method and the six comparison methods on the four benchmark datasets.

4.2.3. Execution efficiency

Tables 1-4 report the attributes of each dynamic network, including the community centers and running time of the STALS. A closer examination of the results reveals that even on the most complex network, the average execution time for the four dynamic network scenarios - Birthdeath, Expandcontract, Hide, and Mergesplit - is remarkly low, with values of 27.99s, 27.80s, 26.08s, and 28.77s, respectively. Notably, the maximum execution time does not exceed 30 seconds, reflecting a high efficiency of the STALS. To put this into perspective, our method outperforms the most efficient method (i.e., Mazza) among the compared six state-of-the-arts, with an average running time of about 31 seconds on a network with 15000 nodes at five snapshots. This is a significant improvement, especially considering the complexity of the networks being analyzed. The efficiency of the STALS algorithm is a testament to its ability to effectively track community structures in dynamic networks, making it a practicable tool.

Table 1 Execution efficiency on Birthdeath dataset.

Timestamps	Nodes	Edges	Community centers	Running time
1	15000	71225	127	2321 ms
2	14581	68539	123	1730 ms
3	13997	65032	131	2103 ms
4	13289	60997	114	1142 ms
5	12781	58558	125	1101 ms

Table 2 Execution efficiency on Expand dataset.

Timestamps	Nodes	Edges	Community centers	Running time
1	15000	71225	127	2065 ms
2	14807	69663	130	1686 ms
3	14711	68305	137	1896 ms
4	13289	60997	114	1142 ms
5	14727	68106	141	1552 ms

Table 3 Execution efficiency on Hide dataset.

Timestamps	Nodes	Edges	Community centers	Running time
1	15000	71225	127	1844 ms
2	13641	64239	111	1458 ms
3	13584	63408	100	1520 ms
4	13707	64019	113	1359 ms
5	13633	63506	133	1645 ms

Table 4 Execution efficiency on Mergesplit dataset.

Timestamps	Nodes	Edges	Community centers	Running time
1	15000	71225	127	1844 ms
2	15000	70290	120	1788 ms
3	15000	69712	125	1701 ms
4	15000	69485	149	2026 ms
5	15000	69086	138	1272 ms

4.3. Experiments on the real-world datasets

4.3.1. Evaluation metric

Modularity is the most commonly used evaluation indicator for measuring the strength of network community structure (Blondel et al., 2008b), which is defined as:

$$Q = \frac{1}{2m}\sum_{xy}[A_{ij} - \frac{k_i k_j}{2m}]\delta(C_i, C_j), \tag{12}$$

Where m is the total number of edges in the network. A_{ij} represents the weight of the edge between nodes i and j. k_i and k_j are the sum of the weights of the edges attached to nodes i and j. $\delta(C_i, C_j) = 1$ if i and

j belong to the same community (i.e., $C_i = C_j$). Otherwise, $\delta(C_i, C_j) = 0$. The ranger of Q is $[-1/2,1]$. The higher of the value of Q, the stronger the detected community structure.

4.3.2. Ablation study

In this section, we perform an ablation experiment to evaluate the impacts of different attribute combinations on model performance, i.e., node curvature (K), node degree (D), spatial proximity (S), TSI (T), and the fast Fourier transform of the TSI (F). By utilizing the EW method, six types of adaptive adjacency matrices were calculated (i.e., KDS, KDF, KSF, DSF, KDST, KDSF).

Fig. 4 visualizes the modularity of the STALS based on the six adaptive adjacency matrices. For both NYC traffic data and Shanghai traffic data, it can be seen that $Q_{KDSF} > Q_{DSF} > Q_{KDF} > Q_{KSF} > Q_{KDST} > Q_{KDS}$. Some findings can be concluded: (i) $Q_{KDST} > Q_{KDS}$ proves that the combination of graph structure and semantic information can improve the modularity. (ii) $Q_{KDSF} > Q_{KDST}$ reveals that the FFT of TSI is more conducive to detecting communities with strong structures, due to its ability to extract inherent structural information of time series. (iii) Q_{KDSF} secures the highest value, whereas Q_{KSF} ranks fourth and Q_{KDS} ranks in fifth in value, emphasizing the superiority of D (i.e., node degree) over the FFT of TSI. (iv) $Q_{DSF} > Q_{KDF}$ highlights that S (i.e., spatial proximity) occupies a higher position than K (i.e., node curvature). Based upon these results, we can conclude the significance of the five attributes for our model: $F > D > S > K$ and $F > T$.

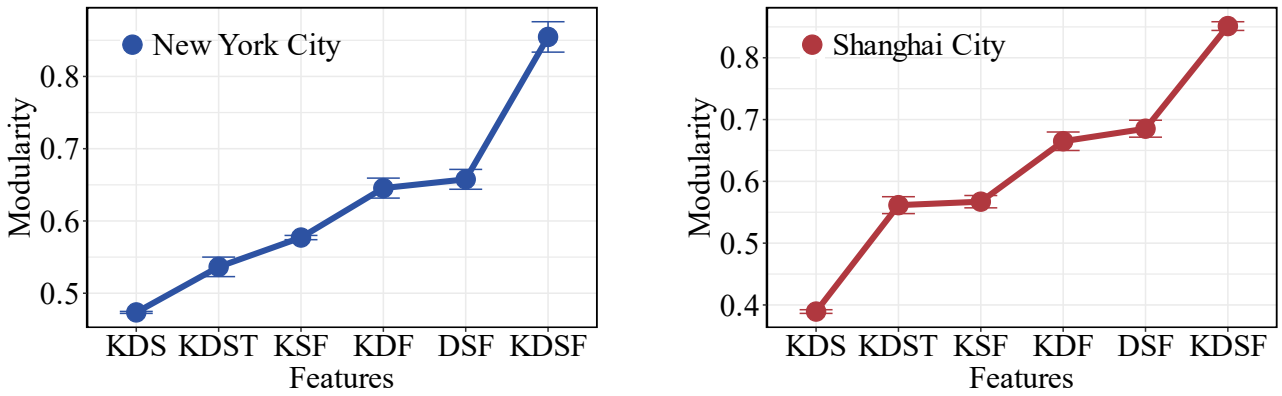

(a) New York City (b) Shanghai City

Fig. 4. Ablation study of the proposed method based on the different feature combinations.

4.3.3. Results

In order to explore the periodicity and sensitivity of congestion propagation, we calculate the transmit of identified communities between different-type days, including weekdays-weekends, weekdays-holidays, and holidays-weekdays. Specifically, the community structures detected by the STALS of each day are merged according to the type of days, and then the same communities between two-type days are counted as the number of community transfers. The results are presented in chord diagrams (**Fig. 5**). The nodes in the outer circle represent community centers, denoted by C-*i* and C-*i*', where $i \in [1, 8]$ represents the level of community centers. For example, C1 represents the primary level of community encompassing the most congested road segment, C2 represents the secondary level, C3 represents the tertiary level, and so forth. Besides, the thickness of the chords is determined by the number of community center transfers, with thicker chords indicating a greater number of transfers.

A comparative analysis of the NYC and Shanghai datasets reveals several key insights: (i) From the perspective of congestion propagation level (i.e. horizontal comparison), most of communities C-*i* on weekdays often evolves into communities C-*i*' at a lower level on non-weekdays, with a small proportion (less than 1/N, N is the total number of transferred community levels) of the communities evolving into higher level. For example, 50% of C1 evolve into C2 and C3, but only less than 10% of those transfers as C-1' in Fig.5a and b. However, this phenomenon is not obvious from holidays to weekdays, which implies that the congestion bottleneck on weekdays after holidays originates from the holidays. (ii) From the perspective of the number of congestion center transfers (i.e. vertical comparison), two intuitive results can be observed. On the one hand, the maximum number of transferred community centers of NYC (i.e., 6) is not much different from that of Shanghai (i.e., 8), revealing the similarity of congestion levels of the two cities. On the other hand, the values of chords in NYC plots (i.e., [0, 200]) are obviously lower than those in Shanghai City (i.e., [0, 1400]), indicating that the congestion frequency of NYC is significantly higher than that of Shanghai City.

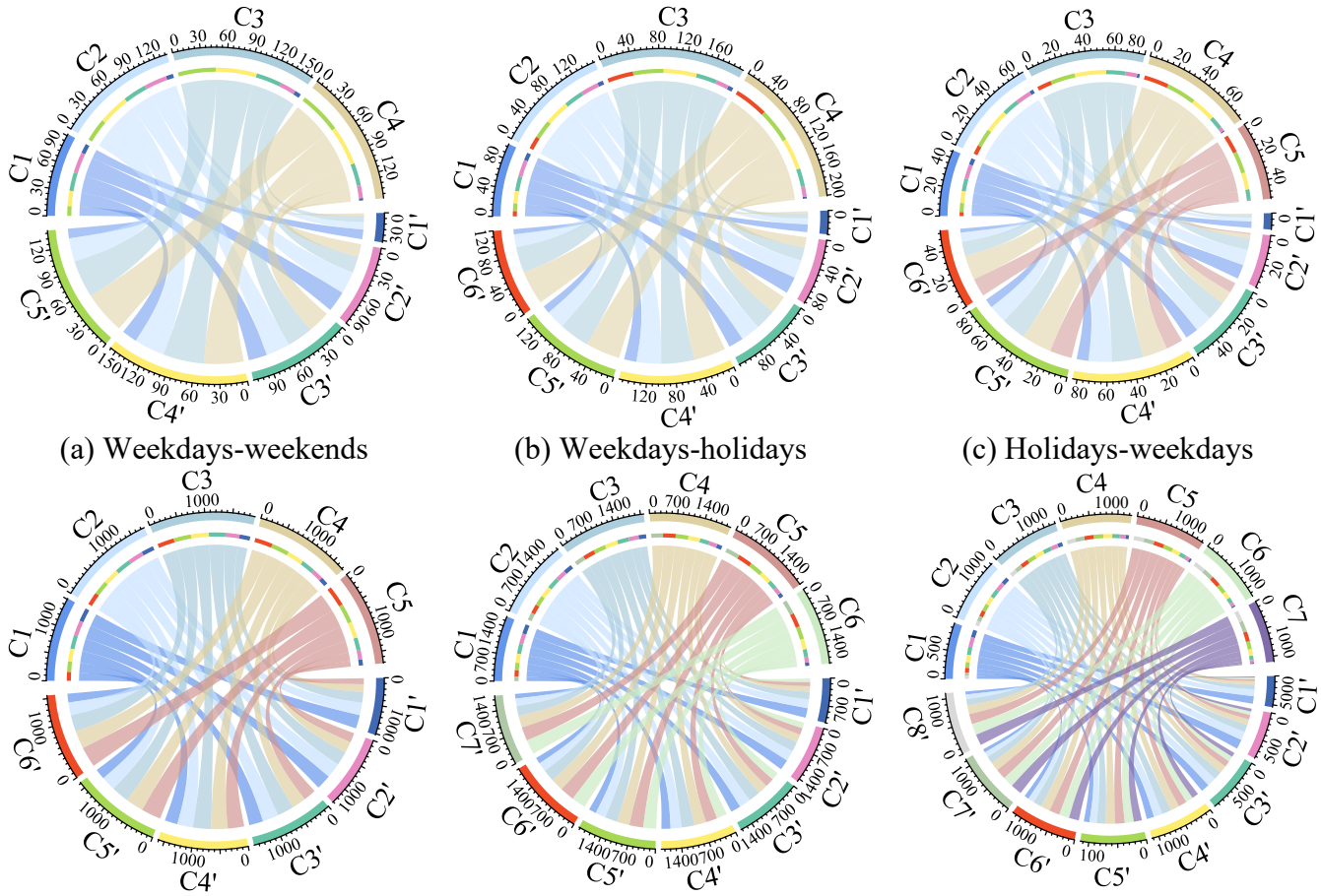

(a) Weekdays-weekends (b) Weekdays-holidays (c) Holidays-weekdays

(d) Weekdays-weekends (e) Weekdays-holidays (f) Holidays-weekdays

Fig. 5. Chord plots showing congestion propagation between different-type days for NYC (**a-c**) and Shanghai city (**d-f**).

To further unveil the correlation between congestion propagation's periodicity with human mobility, we calculate the transmit of identified communities among the peak and off-peak hours over the day. Specifically, the community structures detected by the STALS of each hour are merged according to the type of days (i.e., weekdays, weekends, and holidays), and then the same communities between continuous time periods (i.e., t1, t2, t3, t4, and t5 in **Fig. 5**) are counted as the number of community transfers. Then the numbers are normalized to a ratio p between 0 and 1. The results are visualized in Sankey plots (**Fig. 5**). The nodes in the diagrams represent community centers, denoted by C-i at timestamp t j, where $i \in [1, 11]$ and $j \in [1, 5]$. The size of one node C-i represents the normalized proportion p_i, which is proportional to the thickness of its connected curves. For example, the secondary congestion of NYC on weekdays from 1:00 to 6:00 is more severe than that of primary congestion because the size of C2(t1) is larger than that of C1(t1).

Similarly, our comparative analysis of the NYC and Shanghai datasets also reveals some interesting findings: (i) From the temporal dimension (i.e., horizontal comparison), some congestion propagation mechanism evolving over time can be concluded. Notably, the scale of communities of peak-hours on weekdays for NYC (i.e., 7:00-9:00 and 16:00-19:00) and Shanghai city (i.e., 7:00-9:00 and 17:00-20:00) are growing from bottleneck congestion from 1:00 to 6:00, which is consistent with the human mobility patterns. However, the size of C1(t2) and C1(t4) does not evolve very drastically compared with C1(t1), which implies that the increased human travel usually results in an increase in small-scale communities, but rarely changes the primary communities that cause bottleneck congestion. This rule is also can be observed on weekends and holidays. Besides, comparing the size of communities at t1 and t5, it can be found that the relative proportions of communities at different levels are similar. This also supports the view that congestion levels usually stabilize at a certain level in the evening although experiencing volatile fluctuation at the daytime, which reflects the "self-regulation" of traffic congestion bottlenecks. (ii) From the spatial dimension (i.e., vertical comparison), some common and unique congestion propagation mechanisms for the two cities can be drawn. Overall, NYC and Shanghai city exhibit similar community evolving trend, with community structures more complex at peak hours and relatively simple at off-peak hours, no matter what type of day. Despite the commonality, their congestion bottlenecks are not similar. As one can see, the sizes of C1(t1) and C2(t1) for NYC are usually greater than that of Shanghai. In contrast, the sizes of C3(t1), C4(t1), and even C5(t1) for Shanghai are usually larger than that of NYC. This is an important hint that NYC has more severe congestion bottlenecks than Shanghai, although Shanghai has more small-scale congestion communities at peak hours.

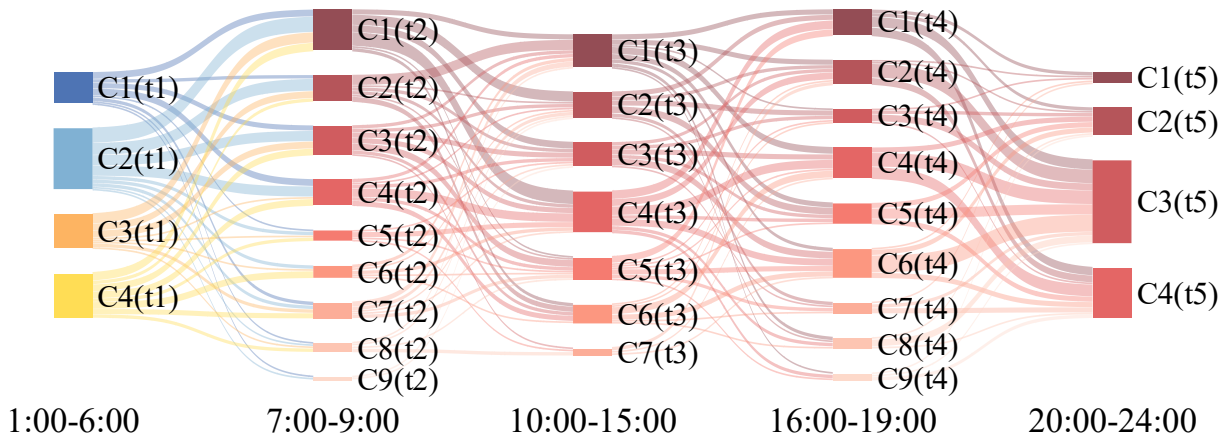

(a) Congestion propagation on weekdays for NYC

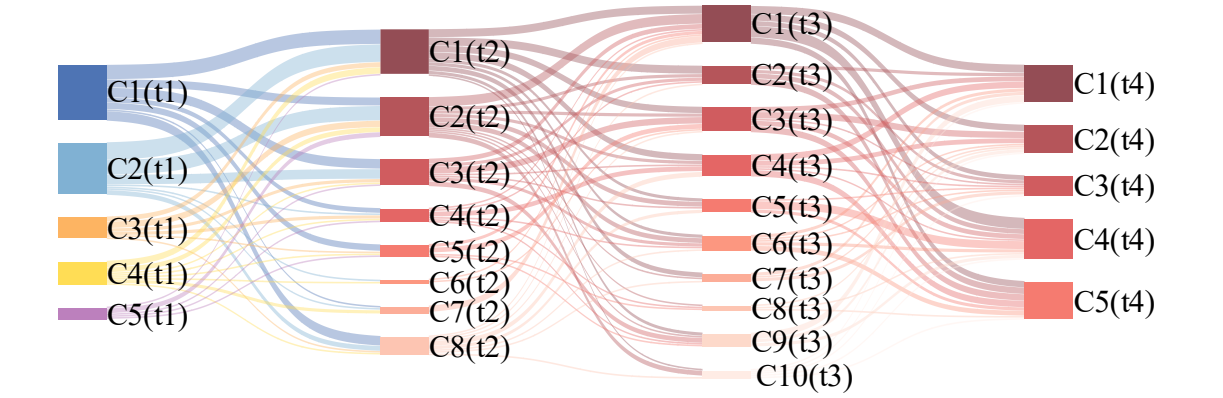

(b) Congestion propagation on weekends for NYC

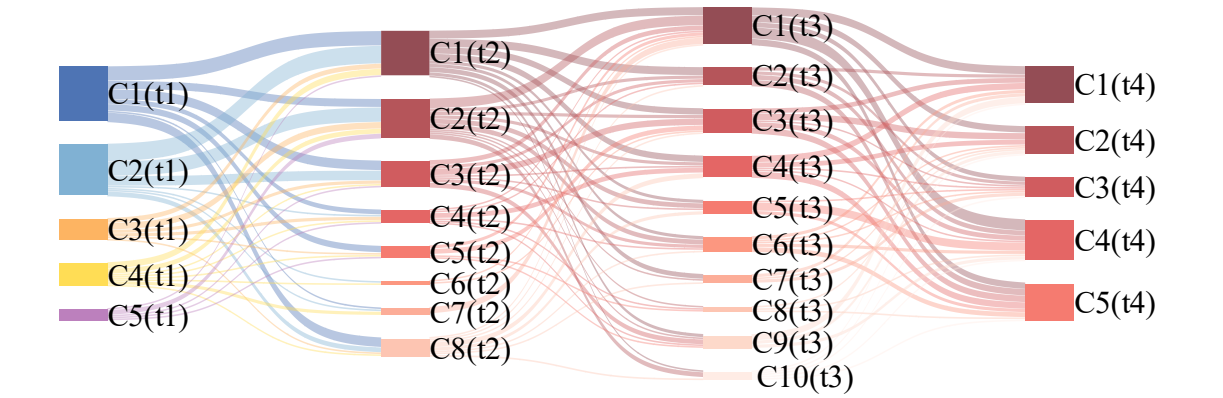

(c) Congestion propagation on holidays for NYC

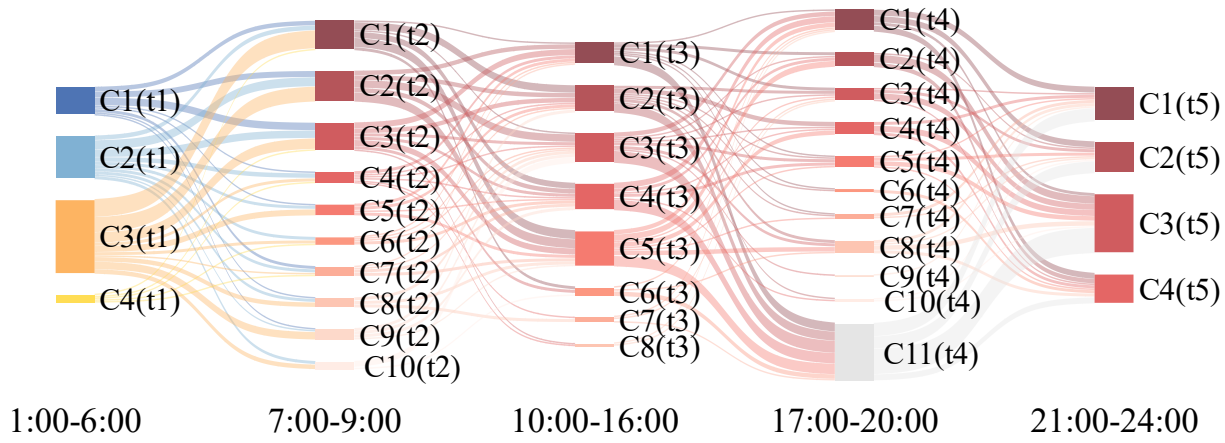

(d) Congestion propagation on weekdays for Shanghai city

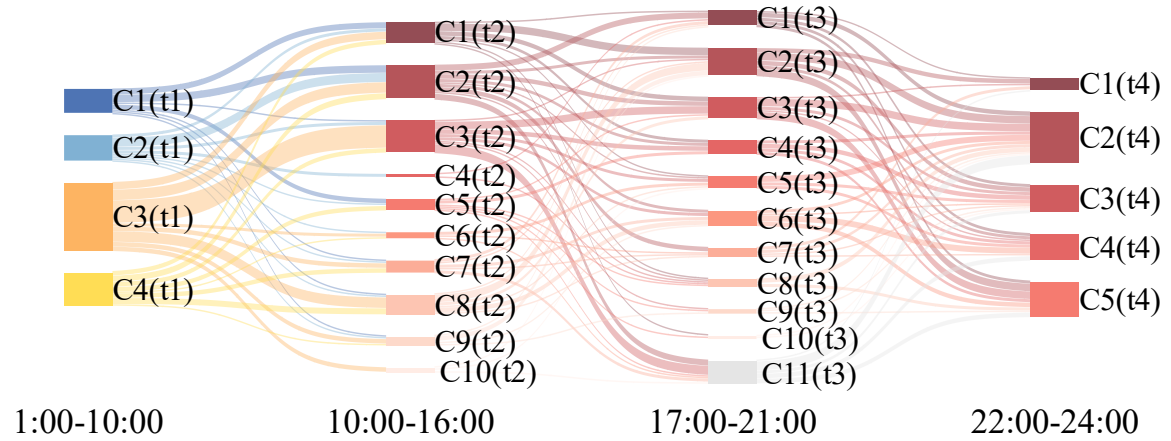

(e) Congestion propagation on weekends for Shanghai city

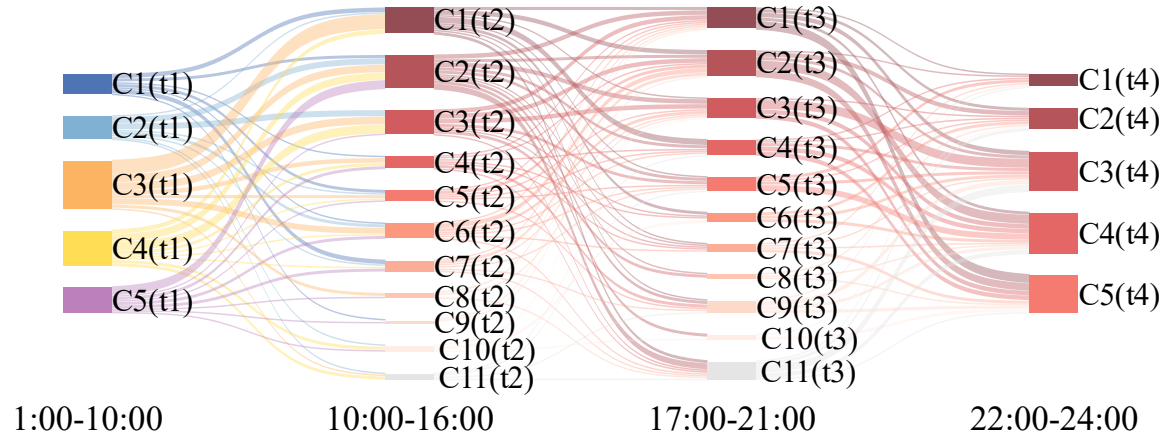

(f) Congestion propagation on holidays for Shanghai city

Fig. 6 Sankey plots showing congestion propagation between time periods in the same-type days for NYC (**a-c**) and Shanghai city(**d-f**).

5. Discussion

5.1. STALS effectiveness implications

Experimental results on the four benchmark-generated networks demonstrate that the STALS exhibits robust community tracking capabilities. The high execution efficiency suggests that the STALS is well-suited for large-scale dynamic network analysis, making it a feasible tool for practitioners. Experiments on the two real-world traffic networks reveal that the community detection method can be successfully applied to congestion propagation analysis, including but not limited to tracking congestion bottlenecks, secondary and tertiary congestion centers in spatiotemporal congestion graphs. The ablation study based on different feature combinations indicates the significance of integrating graph structure and semantic information for its application to traffic congestion analysis. Specifically, the results show that the fusion of node curvature, node degree, spatial proximity, and TSI semantics leads to improvement performance in identifying multi-scale community structures in traffic networks.

To the best of our knowledge, this study is the first to extend community detection to congestion analysis, which is commonly applied to social network and population contact network analysis. Such extension is quite meaningful, as it offers a new perspective on understanding the complex dynamics of traffic flow and congestion propagation at the level of communities. This extension is supported by two key aspects: (i) traffic networks possess similarity with some other complex networks mentioned above when serving as carriers of information transmission; and (ii) communities show targeted advantages than clusters in capturing dynamic changes in network structures, although both can provide coarse-grained descriptions of complex systems and share many conceptual similarities. Specifically, communities not only consider object centers, but also put emphasis on their boundaries. Overall, the proposal and application of our methods are motivated by the underlying values of communities, node relationship, and local search algorithm.

5.2. Traffic congestion propagation mechanism

Taking NYC and Shanghai city as examples, some key findings for traffic congestion propagation mechanism can be drawn: (i) In terms of the congestion propagation patterns on the same type of days, NYC and Shanghai exhibit similar overall trends. Both weekday and weekend peak hours lead to the deterioration of secondary congestion, but the impact of peak hour changes on congestion sources is minimal. In other words, as peak and non-peak hours change, the number of congestion centers fluctuates before stabilizing at a certain level in the evening. So, we can say despite differences in urban landscapes, both cities exhibit striking similarities in their congestion patterns, particularly during peak hours. (ii) When it comes to congestion propagation between different types of days, a fascinating phenomenon emerges. Congestion centers tend to evolve into lower-level congestion centers over time, but holiday-induced congestion exhibits a peculiar persistence, lingering into weekdays like a ghostly presence. This phenomenon suggests that the aftermath of holidays can have a lasting impact on urban traffic, a finding that challenges the conventional wisdom that congestion is solely a weekday concern. (iii) A striking contrast emerges when comparing the two cities. NYC grapples with a more severe bottleneck problem, as evidenced by the proportion of congestion sources and centers. In contrast, Shanghai's complex road network, replete with branches and intersections, gives rise to a significantly higher number of secondary-level congestion centers. This disparity highlights the critical role of urban planning and infrastructure in shaping traffic congestion patterns.

Based on these findings, we try to offer some targeted suggestions for city planners and policymakers. For NYC, focusing on alleviating bottleneck congestion problems is crucial. In Shanghai, a dual approach is necessary, addressing both bottleneck and secondary-level congestion problems, with a particular emphasis on mitigating the effects of narrow and complex road networks. By understanding the intricate interplay between peak hours, road networks, and urban dynamics, we hope both cities create more sustainable transportation systems.

5.3. Limitations and prospects

While our proposed method has demonstrated promising results, there are several avenues for future improvement. Here we identify three key aspects. Firstly, we will attempt to incorporate additional attributes of networks, such as betweenness centrality and closeness centrality, into the dynamic adjacency matrix learning module to enhance the comprehensiveness. This will enable our method to capture a more enhanced representation of the network structure and dynamics. Secondly, although the EW method has shown adaptability in learning weights, it also has some inherent drawbacks, such as reducing the completeness of the relative closeness. Therefore, we aim to explore alternative fusion approaches that can better balance the trade-off between primary and secondary features. Finally, we recognize that the emphasis on local dominance may overlook important global information. To address this, we will investigate ways to integrate global information into our approach, potentially through the use of more advanced optimization techniques or by combining our method with other community detection algorithms that can provide a more comprehensive view of the network structure.

6. Conclusion

This study proposes a novel modular community detection framework, named STALS, to track congestion propagation in dynamic networks. By utilizing the Fourier transform and EW method, a time-varying adjacency matrix can be learned in dynamic networks which is flexible to different granularities. Then, based on local dominance theory, the adaptive matrices are fed into the local search algorithm to search local leaders, identify multi-scale communities, and capture community evolution processes. To the best of our knowledge, this work is among the first efforts to integrate community detection with dynamic road networks to infer traffic congestion propagation.

Such an effort has achieved promising improvements for traffic congestion propagation analysis. The main optimization is to learn the difference of congestion rules from evolving historical data rather than predefined knowledge. Experiments on the four benchmark datasets show that STALS outperforms the state-of-the-art models. Ablation study of two real-world traffic congestion sceneries confirms the

effectiveness of Fourier transform of the TSI and the superiority of multiple attribute combinations (i.e., node curvature, node degree, spatial proximity, and semantic information). A comparative analysis of traffic congestion patterns in NYC and Shanghai reveals intriguing insights into the dynamics of congestion propagation. On weekdays and weekends, peak hours trigger a ripple effect, exacerbating secondary congestion. However, the impact of peak hour fluctuations on congestion sources is surprisingly minimal. As the day unfolds, the number of congestion centers oscillates before stabilizing at a certain level in the evening, much like a self-regulating system. Our findings could provide some targeted policy implications for urban planning and boost urban sustainability.

Declaration of Competing Interest

The author(s) declare no potential conflicts of interest with respect to the research, authorship, and/or publication of this article.

Data availability

The four benchmark datasets can be downloaded from the following website: ML Resources - Dynamic Community Finding.

The average hourly speed data in New York City was downloaded from the Uber Movement in March, 2023. But now, Uber Movement no longer provides this data to the public. We are glad to share this data on request.

Acknowledgements

References

Alam, M. M., Rehman, S., Al-Hadhrami, L. M., & Meyer, J. P. (2014). Extraction of the inherent nature of wind speed using wavelets and FFT. *Energy for Sustainable Development*, 22, 34-47.

Anbaroglu, B., Heydecker, B., & Cheng, T. (2014). Spatio-temporal clustering for non-recurrent traffic congestion detection on urban road networks. *Transportation Research Part C: Emerging Technologies*, 48, 47-65.

Ang, K. L. M., Seng, J. K. P., Ngharamike, E., & Ijemaru, G. K. (2022). Emerging technologies for smart cities' transportation: geo-information, data analytics and machine learning approaches. *ISPRS International Journal of Geo-Information*, 11(2), 85.

Basak, S., Dubey, A., & Bruno, L. (2019, December). Analyzing the cascading effect of traffic congestion using LSTM networks. *In 2019 IEEE International Conference on Big Data (Big Data)* (pp. 2144-2153). IEEE.

Blondel, V. D., Guillaume, J. L., Hendrickx, J. M., de Kerchove, C., & Lambiotte, R. (2008). Local leaders in random networks. *Physical Review E—Statistical, Nonlinear, and Soft Matter Physics*, 77(3), 036114.

Blondel, V. D., Guillaume, J. L., Lambiotte, R., & Lefebvre, E. (2008b). Fast unfolding of communities in large networks. *Journal of statistical mechanics: theory and experiment*, 2008(10), P10008.

Brackstone, M., & McDonald, M. (1999). Car-following: a historical review. *Transportation Research Part F: Traffic Psychology and Behaviour*, 2(4), 181-196.

Bródka, P., Saganowski, S., & Kazienko, P. (2013). GED: the method for group evolution discovery in social networks. *Social Network Analysis and Mining*, 3, 1-14.

Chen, P. (2021). Effects of the entropy weight on TOPSIS. Expert Systems with Applications, 168, 114186.

Chen, Z., Yang, Y., Huang, L., Wang, E., & Li, D. (2018). Discovering urban traffic congestion propagation patterns with taxi trajectory data. *IEEE Access*, 6, 69481-69491.

Daganzo, C.F., (1994). The cell transmission model: A dynamic representation of highway traffic consistent with the hydrodynamic theory. *Transportation Research Part B: Methodological*, 28 (4), 269–287.

Daganzo, C. F. (1995). The cell transmission model, part II: network traffic. *Transportation Research Part B: Methodological*, 29(2), 79-93.

Fan, X., Zhang, J., & Shen, Q. (2019). Prediction of road congestion diffusion based on dynamic Bayesian networks. *In Journal of Physics: Conference Series*, 2 (1176), 022046. IOP Publishing.

Gipps, P. G. (1981). A behavioural car-following model for computer simulation. *Transportation research part B: methodological*, 15(2), 105-111.

Greene, D., Doyle, D., & Cunningham, P. (2010). Tracking the evolution of communities in dynamic social networks. *In 2010 international conference on advances in social networks analysis and mining* (pp. 176-183). IEEE.

Jaccard, P. (1912). The distribution of the flora in the alpine zone. 1. *New phytologist*, 11(2), 37-50.

Jiang, W., & Luo, J. (2022). Graph neural network for traffic forecasting: A survey. *Expert systems with applications*, 207, 117921.

Kipf, T. N., & Welling, M. (2016). Semi-supervised classification with graph convolutional networks. arXiv preprint arXiv:1609.02907.

Kozhabek, A., Chai, W. K., & Zheng, G. (2024). Modeling traffic congestion spreading using a topology-based SIR epidemic model. *IEEE Access*.

Lancichinetti, A., & Fortunato, S. (2009). Benchmarks for testing community detection algorithms on directed and weighted graphs with overlapping communities. *Physical Review E—Statistical, Nonlinear, and Soft Matter Physics*, 80(1), 016118.

Laval, J. A., & Daganzo, C. F. (2006). Lane-changing in traffic streams. *Transportation Research Part B: Methodological*, 40(3), 251-264.

Levin, M. W., & Boyles, S. D. (2016). A multiclass cell transmission model for shared human and autonomous vehicle roads. *Transportation Research Part C: Emerging Technologies*, 62, 103-116.

Liang, M., Liu, R. W., Zhan, Y., Li, H., Zhu, F., & Wang, F. Y. (2022). Fine-grained vessel traffic flow prediction with a spatio-temporal multigraph convolutional network. *IEEE Transactions on Intelligent Transportation Systems*, 23(12), 23694-23707.

Lighthill, M. J., & Whitham, G. B. (1955). On kinematic waves II. A theory of traffic flow on long crowded roads. *Proceedings of the royal society of london. series a. mathematical and physical sciences*, 229(1178), 317-345.

Long, J., Gao, Z., Zhao, X., Lian, A., & Orenstein, P. (2011). Urban traffic jam simulation based on the cell transmission model. *Networks and Spatial Economics*, 11, 43-64.

Lu, J., Li, B., Li, H., & Al-Barakani, A. (2021). Expansion of city scale, traffic modes, traffic congestion,

and air pollution. *Cities*, 108, 102974.

Luan, S., Ke, R., Huang, Z., & Ma, X. (2022). Traffic congestion propagation inference using dynamic Bayesian graph convolution network. *Transportation research part C: emerging technologies*, 135, 103526.

Mazza, M., Cola, G., & Tesconi, M. (2023). Modularity-based approach for tracking communities in dynamic social networks. *Knowledge-Based Systems*, 281, 111067.

Mohammadmosaferi, K. K., & Naderi, H. (2020). Evolution of communities in dynamic social networks: An efficient map-based approach. *Expert Systems with Applications*, 147, 113221.

Narayan, O., & Saniee, I. (2011). Large-scale curvature of networks. *Physical Review E-Statistical, Nonlinear, and Soft Matter Physics*, 84(6), 066108.

Newell, G. F. (1993). A simplified theory of kinematic waves. I: general theory; II: Queuing at freeway bottlenecks; III: Multi-destination flows. *Transportation research part B: methodological*, 27, 281-313.

Nguyen, H., Liu, W., & Chen, F. (2016). Discovering congestion propagation patterns in spatio-temporal traffic data. *IEEE Transactions on Big Data*, 3(2), 169-180.

Rahman, M., Chowdhury, M., Xie, Y., & He, Y. (2013). Review of microscopic lane-changing models and future research opportunities. *IEEE transactions on intelligent transportation systems*, 14(4), 1942-1956.

Ren, Y., Chen, H., Han, Y., Cheng, T., Zhang, Y., & Chen, G. (2020). A hybrid integrated deep learning model for the prediction of citywide spatio-temporal flow volumes. *International Journal of Geographical Information Science*, 34(4), 802-823.

Richards, P. I. (1956). Shock waves on the highway. *Operations research*, 4(1), 42-51.

Saberi, M., Hamedmoghadam, H., Ashfaq, M., Hosseini, S. A., Gu, Z., Shafiei, S., ... & González, M. C. (2020). A simple contagion process describes spreading of traffic jams in urban networks. *Nature communications*, 11(1), 1616.

Shi, D., Shang, F., Chen, B., Expert, P., Lü, L., Stanley, H. E., ... & Li, R. (2024). Local dominance unveils

clusters in networks. *Communications Physics*, 7(1), 170.

Sumalee, A., Zhong, R. X., Pan, T. L., & Szeto, W. Y. (2011). Stochastic cell transmission model (SCTM): A stochastic dynamic traffic model for traffic state surveillance and assignment. *Transportation Research Part B: Methodological*, 45(3), 507-533.

Sun, S., Zhang, C., & Yu, G. (2006). A Bayesian network approach to traffic flow forecasting. *IEEE Transactions on intelligent transportation systems*, 7(1), 124-132.

Sun, J., & Sun, J. (2015). A dynamic Bayesian network model for real-time crash prediction using traffic speed conditions data. *Transportation Research Part C: Emerging Technologies*, 54, 176-186.

Tajeuna, E. G., Bouguessa, M., & Wang, S. (2015). Tracking the evolution of community structures in time-evolving social networks. *In 2015 IEEE International Conference on Data Science and Advanced Analytics (DSAA)* (pp. 1-10). IEEE.

Takaffoli, M., Sangi, F., Fagnan, J., & Zäıane, O. R. (2011). Community evolution mining in dynamic social networks. *Procedia-Social and Behavioral Sciences*, 22, 49-58.

Wang, M., & Debbage, N. (2021). Urban morphology and traffic congestion: Longitudinal evidence from US cities. *Computers, Environment and Urban Systems*, 89, 101676.

Wang, P., Zhang, T., Zheng, Y., & Hu, T. (2022). A multi-view bidirectional spatiotemporal graph network for urban traffic flow imputation. *International Journal of Geographical Information Science*, 36(6), 1231-1257.

Wang, X., Jiang, R., Li, L., Lin, Y., Zheng, X., & Wang, F. Y. (2017). Capturing car-following behaviors by deep learning. *IEEE Transactions on Intelligent Transportation Systems*, 19(3), 910-920.

Wright, C., & Roberg, P. (1998). The conceptual structure of traffic jams. *Transport Policy*, 5(1), 23-35.

Wu, J., Gao, Z., & Sun, H. (2004). Simulation of traffic congestion with SIR model. *Modern Physics Letters B*, 18(30), 1537-1542.

Wu, Z., Pan, S., Chen, F., Long, G., Zhang, C., & Philip, S. Y. (2020). A comprehensive survey on graph neural networks. *IEEE Transactions on Neural Networks and Learning Systems*.

Xiong, H., Zhou, X., & Bennett, D. A. (2023). Detecting spatiotemporal propagation patterns of traffic

congestion from fine-grained vehicle trajectory data. *International Journal of Geographical Information Science*, 37(5), 1157-1179.

Zhang, K., Jia, N., Zheng, L., & Liu, Z. (2019). A novel generative adversarial network for estimation of trip travel time distribution with trajectory data. *Transportation Research Part C: Emerging Technologies*, 108, 223-244.

Zhao, L., Song, Y., Zhang, C., Liu, Y., Wang, P., Lin, T., ... & Li, H. (2019). T-GCN: A temporal graph convolutional network for traffic prediction. *IEEE transactions on intelligent transportation systems*, 21(9), 3848-3858.

Zheng, Q., & Zhang, Y. (2022). DSTAGCN: Dynamic spatial-temporal adjacent graph convolutional network for traffic forecasting. *IEEE Transactions on Big Data*, 9(1), 241-253.